Editors' Suggestion | Featured in Physics

Structured-Pump-Enabled Quantum Pattern Recognition

Xiaodong Qiu, Dongkai Zhang, Wuhong Zhang, and Lixiang Chen*
Department of Physics, Collaborative Innovation Center for Optoelectronic Semiconductors and Efficient Devices, and Jiujiang Research Institute, Xiamen University, Xiamen 361005, China

(Received 7 October 2018; published 26 March 2019)

We report a new scheme of ghost imaging by using a spatially structured pump in the Fourier domain of spontaneous parametric down-conversion for quantum-correlation-based pattern recognition. We exploit the mathematical feature of Laguerre-Gaussian mode's Fourier transform to describe the pump-modulated formation of a ghost image. Of particular interest is the experimental demonstration of a quantum equivalence of a Vander Lugt filter, based on which the nonlocal spiral phase contrast for vortex mapping and quantum-correlation-based human face recognition are implemented successfully. The photons used for probing a test object, scanning the database, and producing a correlation signal can belong to three different light beams, which suggests some security applications where low-light-level illumination and covert operation are desired.

DOI: 10.1103/PhysRevLett.122.123901

Ghost imaging represents an intriguing image acquisition technique in which an image can be reconstructed by using a light beam that never interacts with the object. This phenomenon is somewhat counterintuitive but physically understandable, as either quantum-mechanical or classical correlations are involved [1–4]. The term ghost imaging could be traced to the pioneering work initiated by Shih and co-workers [5], who exploited photon pairs generated via spontaneous parametric down-conversion (SPDC) to realize the first entanglement-based ghost image, following the original proposals by Klyshko [6]. Subsequently, numerous variant schemes, e.g., ghost imaging with classically correlated light or thermal light, and computational ghost imaging, were reported [7–12]. A lot of effort also was focused on modified ghost imaging for seeking novel practical applications. It was demonstrated that sub-shot-noise ghost imaging of weak absorbing objects shows the potential to achieve a larger signal-to-noise ratio than classical imaging methods [13,14]. The study was soon extended to cover the hard-x-ray region, potentially leading to medical imaging with reduced radiation damage [15,16]. A clear, submillimeter ghost image can even be created by using correlated massive particles, e.g., ultracold helium atoms [17]. Recently, a single-photon imaging system with a heralded photon, time-gated, intensified camera was demonstrated as a useful approach for capturing an image of a wasp's wing at very low light levels and for realizing wavelength-transforming ghost imaging [18–20].

In entanglement-based ghost imaging, a fundamental Gaussian pump is routinely used such that it guarantees the high fidelity and quality of the ghost image. But recent years have witnessed a growing interest in structured light engineering [21], which forms the major incentive of our present work to look at how a structured pump, instead of a fundamental Gaussian one, modulates the formation of a ghost image and what new features it can lead to. In addition, previous schemes focused on the near-field region of down-converted crystals, while the far-field region has not yet been fully explored [18,22,23].

Recent years have also witnessed a growing interest in optical pattern recognition, which, unlike using an electronic computer, possesses an inherent capacity for massive parallel processing [24]. This technique could be traced back to the work by Vander Lugt who conducted the first complex spatial filtering [25]. Since then, numerous correlation-based schemes have been realized in various classical optical systems, such as joint transform correlators in linear optics [26], optical correlators based on four-wave mixing in photorefractive medium and atomic vapor [27,28], or those based on a metamaterial beam splitter (BS) [29]. We note that there have also been several attempts, by means of holographic filtering and coincidence detection, at distinguishing among sets of several spatially nonoverlapping objects [30] or identifying geometric features of target objects based on orbital angular momentum (OAM) correlations [31–33]. But these schemes were implemented only with a fundamental Gaussian pump, and the spatial filtering was performed only on the image arm of down-converted light. In this Letter, we explore the structured degrees of freedom of the pump beam to develop a new ghost imaging scheme in the Fourier domain of SPDC. In theory, we adopt the LG modes as the computational basis to describe the pump-modulated ghost imaging, mathematically benefitting from the fact that LG functions are just eigenfunctions of the Fourier transform operator. In experiment, we demonstrate that our scheme can realize a quantum equivalence of the Vander Lugt filter that enables quantum-correlation-based

pattern recognition in situations where low-light-level illumination or covert operation is desired.

In a ghost imaging setup, the object is placed in the idler photon's path, while its ghost image is, nonlocally, recorded in the signal photon's path. Here, we adopt the complete set of normalized Laguerre-Gaussian (LG) modes [34,35] as the computational basis to describe both the object and the image. This adoption is helpful when discussed in the Fourier domain, as it is mathematically beneficial from the fact that LG functions are just eigenfunctions of the Fourier transform operator [36], namely, $\mathcal{F}\{\mathrm{LG}_p^{\ell}(r,\phi)\} = \exp[-i(2p+|\ell|)\pi/2]\mathrm{LG}_p^{\ell}(\rho,\varphi)$, where ℓ and p are the azimuthal and radial indices, respectively, and (r,ϕ) and (ρ,φ) denote real and momentum space, respectively. Instead of using a fundamental Gaussian pump as in a conventional setup, we employ a spatially structured pump beam, described by $\Phi(\rho,\varphi)$, to participating SPDC. Under the thin-crystal approximation and phase-matching condition, we can write the down-converted two-photon state as [37,38]

$$|\Psi\rangle = \sum_{\ell_s,\ell_i,p_s,p_i} C_{p_s,p_i}^{\ell_s,\ell_i}|\ell_s,p_s\rangle|\ell_i,p_i\rangle, \tag{1}$$

where $C_{p_s,p_i}^{\ell_s,\ell_i} = \int \Phi(\rho,\varphi)[\mathrm{LG}_{p_i}^{\ell_i}(\rho,\varphi)]^*[\mathrm{LG}_{p_s}^{\ell_s}(\rho,\varphi)]^*\rho d\rho d\varphi$ denotes the probability amplitude of finding the signal photon in the mode of $\mathrm{LG}_{p_s}^{\ell_s}$ and the idler one in $\mathrm{LG}_{p_i}^{\ell_i}$. Similarly, owing to the orthogonality and completeness of the LG mode basis, we can expand the complex transmission function of the object as $O(r,\phi) = \sum_{\ell_o,p_o} A_{\ell_o,p_o}\mathrm{LG}_{\ell_0,p_0}\times(r,\phi)$, where $A_{\ell_o,p_o} = \int [\mathrm{LG}_{\ell_o,p_o}(r,\phi)]^* O(r,\phi) r dr d\phi$ [35]. The idler photons are directed to illuminate the objects, which are subsequently collected by a lens and coupled into a single-mode fiber (SMF). In a back-projection picture, we can equivalently consider that the fundamental Gaussian mode derived from SMF, after being expanded by the collecting lens, goes back to illuminate the object. We estimate the beam waist of the expanded Gaussian mode as approximately 2.2 mm, sufficiently larger than the dimension of the object of approximately 1.0 mm. Thus, such a projective measurement inversely projects the idler photons onto a conjugated state (to the object's transmission function), i.e., $|\psi\rangle_i = \sum_{\ell_i,p_i} A_{\ell_i,p_i}^*|-\ell_i,p_i\rangle$ [39]. In our scheme, both the object and the intensified CCD (ICCD) camera are positioned at the Fourier plane of a down-converted crystal. Equivalently, the idler photons at the crystal are projected onto [40]

$$|\psi'\rangle_i = \sum_{\ell_i,p_i} A_{\ell_i,p_i}^* \exp[i(2p_i+|\ell_i|)\pi/2]|-\ell_i,p_i\rangle, \tag{2}$$

i.e., $|\psi'\rangle_i = \mathcal{F}^{-1}|\psi\rangle_i$. By combining Eq. (2) with Eq. (1), we know that the signal photon at the plane of the ICCD camera acquires the state

$$\begin{aligned}|\psi\rangle_s &= \mathcal{F}|\psi'\rangle_s = \mathcal{F}\langle\psi_i'|\Psi\rangle \\ &= \sum_{\ell_s,\ell_i,p_s,p_i} A_{\ell_i,p_i} C_{p_s,p_i}^{\ell_s,-\ell_i} \exp[-i(2p_i+2p_s+|\ell_i|+|\ell_s|)\pi/2]|\ell_s,p_s\rangle,\end{aligned} \tag{3}$$

which just describes how a structured pump affects the formation of a ghost image via the two-photon amplitude $C_{p_s,p_i}^{\ell_s,\ell_i}$. Note that the mathematical feature of the LG function's Fourier transform has been utilized in both Eqs. (2) and (3). For the particular case with a fundamental Gaussian pump of sufficiently large beam waist, we have $C_{p_s,p_i}^{\ell_s,\ell_i} = \delta_{\ell_s,-\ell_i}\delta_{p_s,p_i}$ so Eq. (3) can be simply reduced to $|\psi\rangle_s = \sum_{\ell_s,p_s} A_{\ell_s,p_s}\exp(i\ell_s\pi)|\ell_s,p_s\rangle$, which describes an inverted ghost image of the object, i.e., $I(r,\phi) = |O(r,\phi+\pi)|^2$. Generally, after some algebra [40], we can translate the state described by Eq. (3) into a two-dimensional complex function,

$$\begin{aligned}\psi_s(r,\phi) &= \mathcal{F}\left\{\sum_{\ell_s,\ell_i,p_s,p_i} A_{\ell_i,p_i} C_{p_s,p_i}^{\ell_s,-\ell_i} \exp[-i(2p_i+|\ell_i|)\pi/2]\mathrm{LG}_{\ell_s,p_s}(\rho,\varphi)\right\} \\ &= \tilde{\Phi}(r,\phi)\otimes O(r,\phi+\pi),\end{aligned} \tag{4}$$

where $\otimes$ denotes convolution and $\tilde{\Phi}(r,\phi)$ represents the Fourier spectrum of the pump field. The above equation also suggests a particularly interesting way to realize quantum-correlation-based pattern recognition: If we use a light field carrying the Fourier spectrum of the conjugate object to serve as the pump beam, the ghost image will simply appear as a correlation signal because of the quantum equivalence of the Vander Lugt filter constructed in the Fourier domain of SPDC. Here, we build such a setup and demonstrate nonlocal spiral phase contrast for vortex mapping and quantum-correlation-based human face recognition.

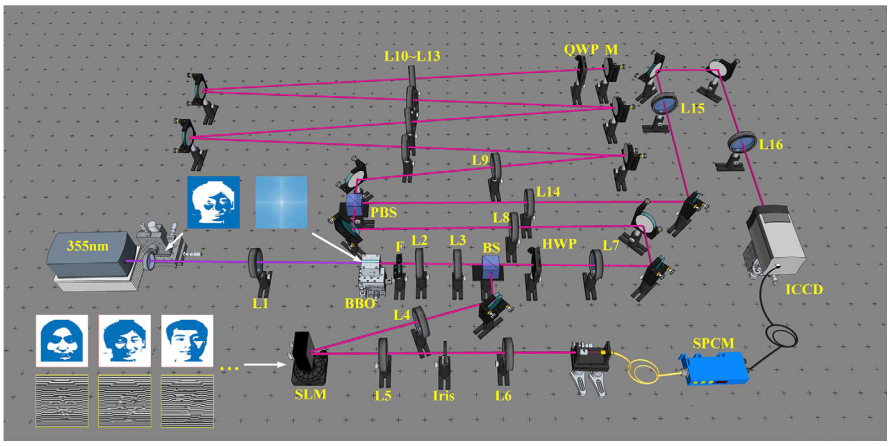

FIG. 1. Schematic illustration of the experimental setup. See Supplemental Material [40] for full details.

Our optical system is sketched in Fig. 1, in which the spatially structured pump is distinguished from the conventional setup of a fundamental Gaussian pump [18]. The fundamental Gaussian pump beam is initially derived from a 355-nm ultraviolet (UV) laser; then, it is imparted with a desired modulation before pumping a 3-mm-long β-barium borate (BBO) crystal. Next, photon pairs of degenerate wavelength at 710 nm are generated via type-I SPDC and separated by a 50:50 nonpolarizing BS. The reflected idler photons are directed to illuminate the spatial light modulator (SLM) that displays the holographic gratings carrying both the amplitude and phase of the object. Then, the first diffraction order acquires the object's complex amplitude, which is subsequently filtered out and coupled into a SMF connected to a single-photon counting module (SPCM). Meanwhile, single-photon events from SPCM serve as the trigger signal for the ICCD camera operating in direct gate mode. We work with a region of interest of 256×256 pixels, covering an area of 3.328×3.328 mm^2. Each image is obtained by summing several frames, with an exposition time of 2 s for each frame. Remember that both the SLM and ICCD cameras are positioned at the Fourier plane of the BBO crystal, and an optical delay of about 20.8 meters is requested in the image arm to compensate for the electronic delay (see Supplemental Material [40] for full details).

Another feature of a $\mathrm{LG}_{\ell,p}$ beam is its characteristic helical phase fronts that endow each photon with $\ell\hbar$ OAM or a vortex with a topological charge ℓ [34]. Recently, OAM or vortex beams have received intense research interest, ranging from optical communications and micromanipulation to quantum information [43]. In these applications, efficient vortex detection is of fundamental importance. Here, we demonstrate that optical vortices can be nonlocally mapped and measured via our system with a single-vortex pump. For this, we impart the Gaussian UV light with a spiral phase front of $\exp(-i\phi)$ by passing it through a vortex phase plate (VPP, RPC Photonics); we then pump the BBO crystal in the Fourier domain. As shown by the first column of Fig. 2, we display the holographic gratings in the SLM to generate several optical vortices, which are written as $O(r,\phi) = \sum_j A(r_j)\exp(i\phi_j)$, with (r_j, φ_j) denoting the local transverse coordinates with respect to the center of the jth vortex. If a fundamental Gaussian pump is used, we merely observe several dark cores embedded in the bright background (see the second and third columns of Fig. 2). Instead, if a vortex pump is employed, according to Eq. (4), we know that the resultant patterns recorded by the ICCD camera will become $\psi_s(r,\phi) = \mathcal{F}[\exp(-i\varphi)] \otimes (\sum_j A(r_j)\exp(i\phi_j))$, which is, in essence, mathematically related to the concept of spiral phase contrast [44,45]. As a result, only the dark cores, i.e., the singular areas of each vortex, can be nonlocally highlighted, as they

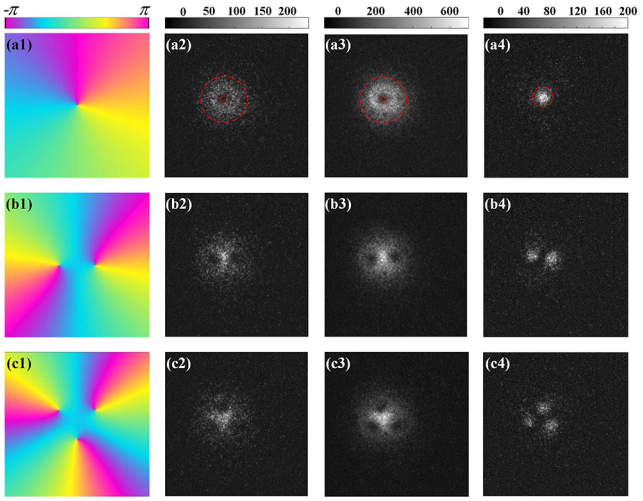

FIG. 2. Experimental results for nonlocal vortex mapping. First column: Vortices displayed by the SLM. Second and third columns: Ghost images created by summing 20 frames and 100 frames, respectively. Fourth column: Bright spots revealing the dark cores of each vortex after nonlocal mapping with 20 frames. The gray-scale bar is in units of photons/pixel.

can be considered as a special type of extremely discontinuous edge. We present our observations in the fourth column of Fig. 2, from which one can see several bright spots appearing in contrast to the dark background, clearly revealing the location of each vortex. Our scheme is conceptually new and evidently distinguished from previous schemes that used a classical light beam [46,47], as here we employ the vortex pump to act as the nonlocal spiral phase filter via SPDC and exploit twin photons of quantum correlations to implement the spiral phase contrast. For a quantitative comparison, we use a contrast-to-noise ratio, $\mathrm{CNR} = (\langle G_{\mathrm{in}}\rangle - \langle G_{\mathrm{out}}\rangle)/\sqrt{\sigma_{\mathrm{in}}^2 + \sigma_{\mathrm{out}}^2}$, to characterize the visibility of the recorded images [48], where $\langle G_{\mathrm{in}}\rangle$ and $\langle G_{\mathrm{out}}\rangle$ represent the ensemble average of the signal at any pixel inside and outside the contours of the desired images, respectively, and σ_{in}^2 and σ_{out}^2 are the variances. As marked by the dashed outlines in Figs. 2(a2), 2(a3), and 2(a4), the image is a doughnut-shaped vortex, while it is a Gaussian spot for the correlation signal. We calculate the CNR of vortex images as 1.12 and 1.53 for Figs. 2(a2) and 2(a3) by summing 20 and 100 frames, respectively. In contrast, the CNR of the correlation signal in Fig. 2(a4) can reach 1.78 with 20 frames only. In other words, our scheme can achieve a clear signal of a higher CNR even with fewer frames, thus effectively reducing the recognition time.

The human face plays a very important role in our social interaction and in conveying a person's identity. From a practical point of view, face recognition, as one of the biometric recognition processes, is highly desirable in a wide variety of security applications [49]. Based on correlation algorithms, much work has been conducted to combine the conception of optical correlation with other spatial-domain recognition methods, aiming to achieve new face recognition algorithms with higher discrimination and robustness characteristics [50]. In the face recognition method, a sample face is compared with a set of known faces stored in a database. For the purpose of this demonstration, we capture the facial photographs, with a commercial digital camera, of five different people who are currently working in our laboratory. The facial photographs are subsequently conjugated and binarized, with each pixel being assigned a phase value of 0 or π accordingly. Then, the phase information of the pixels is transferred to several pure-phase samples. To impart the spatial frequency information of the sample faces onto the pump beam, we direct the fundamental Gaussian UV light to illuminate the samples and position the BBO crystal just at the Fourier plane of the Fourier lens. Here, the spatially modulated pump beam can be considered again as the quantum equivalence of the Vander Lugt filter, as it bridges the quantum correlations established between down-converted photon pairs in the Fourier domain. Thus, according to Eq. (4), we can expect a sharp correlation peak as the signature of a match, i.e., successful face recognition. In our experiment, we prepare the pump beam to bear the frequency information of a specific sample face; then, we scan the known faces by loading them sequentially on the SLM. The correlation signals for 5×5 different face combinations are recorded separately by a ICCD camera and shown together in Fig. 3. Strong correlation peaks are observed, as expected, appearing along the diagonal line of the measured cross-correlation matrix. However, we also observe several weak correlation signals in the nondiagonal elements, which characterize the slight similarity between the faces of two different people. Thus, our quantum-correlation-based face recognition can be achieved after comparing the correlation signals with a threshold that is adjusted for a chosen security level.

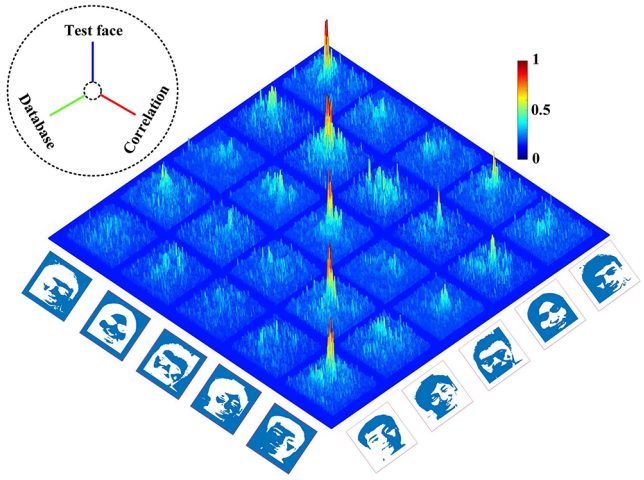

FIG. 3. Experimental results for human face recognition. The test photographs (left axis) are binarized in phase and imparted to the UV light; they are then Fourier transformed to participating SPDC. For each test photograph, the five reference photographs (right axis) are scanned by loading them sequentially in the SLM. Correlation signals for 5×5 combinations are recorded by summing 20 frames with the ICCD camera. The top-left inset suggests the potential in covert imaging: The photons for probing the sample face, scanning the face database, and producing the correlation signal belong to three different light beams.

In summary, based on a modified ghost imaging setup with a spatially structured pump and a time-gated ICCD camera, we have constructed a quantum equivalence of the Vander Lugt filter and demonstrated a new pattern recognition for nonlocal vortex mapping and human face recognition. It is apparent that the acquisition of a correlation peak is more efficient than that of a structured object, as the latter generally needs many frames and is time-consuming. Thus, illumination with a reduced photon flux can avoid letting the tested object become aware of its detection, which is potentially useful for covert illumination. In addition, we have readily encoded the spatial spectrum of reference onto a two-photon wave function via the structured pump, where the idler photons illuminate the tested object while signal photons are used to produce the correlation signal nonlocally. Thus, one should possess both the signal photons and the preknowledge of reference

to accomplish the object identification, which could be useful to avoid optical eavesdropping for security applications. It is also challenging to fully align the optical system, particularly for our 20.8-m image-preserving delay line. In addition, a better time and spatial overlap of both the Fourier planes of the camera and the object with the pump profile at the BBO crystal is highly desirable, which could further improve the visibility. We also anticipate that the flexibility of our scheme can be further improved if we have another SLM that can work in the UV regime to modulate the pump beam. By introducing artificial neutral network techniques such as deep learning [51] into our present system, we may develop a hybrid optical or digital architecture for diverse face recognition. Also, our method could be extended to the case of pseudothermal ghost imaging by spatially modulating the classical light source. Regardless of an increased background noise level, it may work at multiple wavelengths and may realize the colored object identification [52]. We leave these possibilities to future studies.

We are grateful to Miles Padgett at the University of Glasgow for kind support, and thank IMNST at Xiamen University and Yujie Chen at Sun Yat-sen University for fabricating some of the samples, Baoqing Sun at Shandong University for helpful discussions, and Jiguo Wang, Weidong Yang, Changshun Xiao, and Ting Wang for supplying their facial photographs. This work is supported by the National Natural Science Foundation of China (Grant No. 91636109), the Fundamental Research Funds for the Central Universities at Xiamen University (Grant No. 20720160040), the Natural Science Foundation of Fujian Province of China for Distinguished Young Scientists (Grant No. 2015J06002), and the program for New Century Excellent Talents in University of China (Grant No. NCET-13-0495).

*chenlx@xmu.edu.cn

[1] L. A. Lugiato, A. Gatti, and E. Brambilla, Quantum imaging, J. Opt. B **4**, S176 (2002).
[2] M. D'Angelo and Y. H. Shih, Quantum imaging, Laser Phys. Lett. **2**, 567 (2005).
[3] B. I. Erkmen and J. H. Shapiro, Ghost imaging: From quantum to classical to computational, Adv. Opt. Photonics **2**, 405 (2010).
[4] P. A. Moreau, E. Toninelli, T. Gregory, and M. J. Padgett, Ghost imaging using optical correlations, Laser Photonics Rev. **12**, 1700143 (2018).
[5] T. B. Pittman, Y. H. Shih, D. V. Strekalov, and A. V. Sergienko, Optical imaging by means of two-photon quantum entanglement, Phys. Rev. A **52**, R3429 (1995).
[6] D. Klyshko, Combine EPR and two-slit experiments: Interference of advanced waves, Phys. Lett. A **132**, 299 (1988).
[7] R. S. Bennink, S. J. Bentley, and R. W. Boyd, "Two-Photon" Coincidence Imaging with a Classical Source, Phys. Rev. Lett. **89**, 113601 (2002).
[8] R. S. Bennink, S. J. Bentley, R. W. Boyd, and J. C. Howell, Quantum and Classical Coincidence Imaging, Phys. Rev. Lett. **92**, 033601 (2004).
[9] A. Valencia, G. Scarcelli, M. D'Angelo, and Y. Shih, Two-Photon Imaging with Thermal Light, Phys. Rev. Lett. **94**, 063601 (2005).
[10] F. Ferri, D. Magatti, A. Gatti, M. Bache, E. Brambilla, and L. A. Lugiato, High-Resolution Ghost Image and Ghost Diffraction Experiments with Thermal Light, Phys. Rev. Lett. **94**, 183602 (2005).
[11] J. H. Shapiro, Computational ghost imaging, Phys. Rev. A **78**, 061802(R) (2008).
[12] Y. Altmann, S. McLaughlin, M. J. Padgett, V. K Goyal, A. O. Hero, and D. Faccio, Quantum-inspired computational imaging, Science **361**, eaat2298 (2018).
[13] G. Brida, M. Genovese, and I. Ruo Berchera, Experimental realization of sub-shot-noise quantum imaging, Nat. Photonics **4**, 227 (2010).
[14] N. Samantaray, I. Ruo Berchera, A. Meda, and M. Genovese, Realization of the first sub-shot-noise wide field microscope, Light Sci. Appl. **6**, e17005 (2017).
[15] D. Pelliccia, A. Rack, M. Scheel, V. Cantelli, and D. M. Paganin, Experimental X-ray Ghost Imaging, Phys. Rev. Lett. **117**, 113902 (2016).
[16] H. Yu, R. Lu, S. Han, H. Xie, G. Du, T. Xiao, and D. Zhu, Fourier-Transform Ghost Imaging with Hard X Rays, Phys. Rev. Lett. **117**, 113901 (2016).
[17] R. I. Khakimov, B. M. Henson, D. K. Shin, S. S. Hodgman, R. G. Dall, K. G. H. Baldwin, and A. G. Truscott, Ghost imaging with atoms, Nature (London) **540**, 100 (2016).
[18] R. S. Aspden, D. S. Tasca, R. W. Boyd, and M. J. Padgett, EPR-based ghost imaging using a single-photon-sensitive camera, New J. Phys. **15**, 073032 (2013).
[19] P. A. Morris, R. S. Aspden, J. E. C. Bell, R. W. Boyd, and M. J. Padgett, Imaging with a small number of photons, Nat. Commun. **6**, 5913 (2015).
[20] R. S. Aspden, N. R. Gemmell, P. A. Morris, D. S. Tasca, L. Mertens, M. G. Tanner, R. A. Kirkwood, A. Ruggeri, A. Tosi, R. W. Boyd, G. S. Buller, R. H. Hadfield, and M. J. Padgett, Photon-sparse microscopy: Visible light imaging using infrared illumination, Optica **2**, 1049 (2015).
[21] H. Rubinsztein-Dunlop *et al.*, Roadmap on structured light, J. Opt. **19**, 013001 (2017).
[22] J. C. Howell, R. S. Bennink, S. J. Bentley, and R. W. Boyd, Realization of the Einstein-Podolsky-Rosen Paradox Using Momentum- and Position-Entangled Photons from Spontaneous Parametric Down Conversion, Phys. Rev. Lett. **92**, 210403 (2004).
[23] M. D'Angelo, Y.-H. Kim, S. P. Kulik, and Y. Shih, Identifying Entanglement Using Quantum Ghost Interference and Imaging, Phys. Rev. Lett. **92**, 233601 (2004).
[24] *Real-Time Optical Information Processing*, edited by B. Javidi and J. L. Horner (Academic Press, New York, 1994).
[25] A. VanderLugt, Signal detection by complex spatial filtering, IEEE Trans. Inf. Theory **10**, 139 (1964).
[26] C. S. Weaver and J. W. Goodman, A technique for optically convolving two functions, Appl. Opt. **5**, 1248 (1966).

[27] B. L. Volodin, B. Kippelen, K. Meerholz, B. Javidi, and N. Peyghambarian, A polymeric optical pattern-recognition system for security verification, Nature (London) **383**, 58 (1996).
[28] I. Biaggio, J. P. Partanen, B. Ai, R. J. Knize, and R. W. Hellwarth, Optical image processing by an atomic vapour, Nature (London) **371**, 318 (1994).
[29] M. Papaioannou, E. Plum, and N. I. Zheludev, All-optical pattern recognition and image processing on a metamaterial beam splitter, ACS Photonics **4**, 217 (2017).
[30] M. Malik, H. Shin, M. O'Sullivan, P. Zerom, and R. W. Boyd, Quantum Ghost Imaging Identification with Correlated Photon Pairs, Phys. Rev. Lett. **104**, 163602 (2010).
[31] B. Jack, J. Leach, J. Romero, S. Franke-Arnold, M. Ritsch-Marte, S. M. Barnett, and M. J. Padgett, Holographic Ghost Imaging and the Violation of a Bell Inequality, Phys. Rev. Lett. **103**, 083602 (2009).
[32] N. Uribe-Patarroyo, A. Fraine, D. S. Simon, O. Minaeva, and A. V. Sergienko, Object Identification Using Correlated Orbital Angular Momentum States, Phys. Rev. Lett. **110**, 043601 (2013).
[33] L. Chen, J. Lei, and J. Romero, Quantum digital spiral imaging, Light Sci. Appl. **3**, e153 (2014).
[34] L. Allen, M. W. Beijersbergen, R. J. C. Spreeuw, and J. P. Woerdman, Orbital angular momentum of light and the transformation of Laguerre-Gaussian laser modes, Phys. Rev. A **45**, 8185 (1992).
[35] L. Torner, J. P. Torres, and S. Carrasco, Digital spiral imaging, Opt. Express **13**, 873 (2005).
[36] L. Yu, W. Huang, M. Huang, Z. Zhu, X. Zeng, and W. Ji, The Laguerre-Gaussian series representation of two-dimensional fractional Fourier transform, J. Phys. A **31**, 9353 (1998).
[37] S. P. Walborn, C. H. Monken, S. Padua, and P. H. Souto Ribeiro, Spatial correlations in parametric downconversion, Phys. Rep. **495**, 87 (2010).
[38] A. M. Yao, Angular momentum decomposition of entangled photons with an arbitrary pump, New J. Phys. **13**, 053048 (2011).
[39] A. Mair, A. Vaziri, G. Weihs, and A. Zeilinger, Entanglement of the orbital angular momentum states of photons, Nature (London) **412**, 313 (2001).
[40] See Supplemental Material at http://link.aps.org/supplemental/10.1103/PhysRevLett.122.123901 for derivation of Eq. (4) and full experimental details, which includes Refs. [41,42].
[41] H. Qassim, F. M. Miatto, J. P. Torres, M. J. Padgett, E. Karimi, and R. W. Boyd, Limitations to the determination of a Laguerre-Gauss spectrum via projective, phase-flattening measurement, J. Opt. Soc. Am. B **31**, A20 (2014).
[42] F. Bouchard, N. H. Valencia, F. Brandt, R. Fickler, M. Huber, and M. Malik, Measuring azimuthal and radial modes of photons, Opt. Express **26**, 31925 (2018).
[43] M. J. Padgett, Orbital angular momentum 25 years on, Opt. Express **25**, 11265 (2017).
[44] S. Frhapter, A. Jesacher, S. Bernet, and M. Ritsch-Marte, Spiral phase contrast imaging in microscopy, Opt. Express **13**, 689 (2005).
[45] M. Ritsch-Marte, Orbital angular momentum light in microscopy, Phil Trans. R. Soc. A **375**, 20150437 (2017).
[46] R. Steiger, S. Bernet, and M. Ritsch-Marte, Mapping of phase singularities with spiral phase contrast microscopy, Opt. Express **21**, 16282 (2013).
[47] W. Zhang, J. Wang, F. Li, L. Chen, and E. Karimi, Revealing optical vortices with a small number of photons, Laser Photonics Rev. **11**, 1600163 (2017).
[48] P. Zerom, Z. Shi, M. O'Sullivan, K. Chan, M. Krogstad, J. Shapiro, and R. Boyd, Thermal ghost imaging with averaged speckle patterns, Phys. Rev. A **86**, 063817 (2012).
[49] M. S. Millan, Advanced optical correlation and digital methods for pattern matching—50th anniversary of Vander Lugt matched filter, J. Opt. **14**, 103001 (2012).
[50] B. V. K. V. Kumar, M. Savvides, and C. Xie, Correlation pattern recognition for face recognition, Proc. IEEE **94**, 1963 (2006).
[51] Q. Wang, A. Alfalou, and C. Brosseau, New perspectives in face correlation research: A tutorial, Adv. Opt. Photonics **9**, 1 (2017).
[52] D. Duan, S. Du, and Y. Xia, Multiwavelength ghost imaging, Phys. Rev. A **88**, 053842 (2013).